Computer Analysis of Reinforced Concrete Sections Under Combined Bending and Compression

Analyse de sections en béton armé soumises à un effort normal avec flexion au moyen d'un calculateur électronique

Computer-Berechnung von Stahlbetonquerschnitten unter kombinierter Biegung und Druck

S. K. GHOSH
Adjunct Professor of Civil Engineering

M. Z. COHN
M. IABSE, Professor of Civil Engineering

University of Waterloo, Waterloo, Ontario, Canada

Introduction

The load-deformation characteristics of a reinforced concrete section subject to combined bending and axial load is significantly different from that of a section under pure flexure. The most critical difference may be the drastic reduction in sectional ductility which is caused by the presence of axial load.

Approximate load-moment interaction diagrams based on both the working stress [1] and ultimate strength [2] design theories are available for the design of square, rectangular and circular sections. However, the behaviour of reinforced concrete sections subject to combined bending and axial load in its generality, has been studied only to a very limited extent [3]–[8].

The purpose of this paper is to present some results of a comprehensive investigation into the subject [9]. In addition to providing a better understanding of inelastic action in reinforced concrete columns, these results suggest conditions under which inelastic analysis and design methods may be considered applicable to these members.

405 symmetrically reinforced rectangular concrete sections of identical dimensions, Fig. 1, but with varying *concrete strengths*, *steel grades*, and *reinforcement percentages*, and subject to varying *magnitudes of axial load* (Table 1), were analysed by using the sectional theory and the numerical method described in [8]. Reliable representations of the stress-strain properties of concrete and steel, proposed by SARGIN [10] and also described in [8], were

Table 1. Geometric and material properties of sections analysed

P/P_u =0.0	P/P_u =0.1	P/P_u =0.2	P/P_u =0.3	P/P_u =0.4	P/P_u =0.45	P/P_u =0.5	P/P_u =0.6	P/P_u =0.8	f'_c ksi	f'_c ksi	$p=p'$ %
Section no.											
1	46	91	136	181	226	271	316	361			0.5
2	47	92	137	182	227	272	317	362			1.0
3	48	93	138	183	228	273	318	363		45	1.5
4	49	94	139	184	229	274	319	364			2.0
5	50	95	140	185	230	275	320	365			3.0
6	51	96	141	186	231	276	321	366			0.5
7	52	97	142	187	232	277	322	367			1.0
8	53	98	143	188	233	278	323	368	3	60	1.5
9	54	99	144	189	234	279	324	369			2.0
10	55	100	145	190	235	280	325	370			3.0
11	56	101	146	191	236	281	326	371			0.5
12	57	102	147	192	237	282	327	372			1.0
13	58	103	148	193	238	283	328	373		75	1.5
14	59	104	149	194	239	284	329	374			2.0
15	60	105	150	195	240	285	330	375			3.0
16	61	106	151	196	241	286	331	376			0.5
17	62	107	152	197	242	287	332	377			1.0
18	63	108	153	198	243	288	333	378		45	1.5
19	64	109	154	199	244	289	334	379			2.0
20	65	110	155	200	245	290	335	380			3.0
21	66	111	156	201	246	291	336	381			0.5
22	67	112	157	202	247	292	337	382			1.0
23	68	113	158	203	248	293	338	383	4	40	1.5
24	69	114	159	204	249	294	339	384			2.0
25	70	115	160	205	250	295	340	385			3.0
26	71	116	161	206	251	296	341	386			0.5
27	72	117	162	207	252	297	342	387			1.0
28	73	118	163	208	253	298	343	388		75	1.5
29	74	119	164	209	254	299	344	389			2.0
30	75	120	165	210	255	300	345	390			3.0
31	76	121	166	211	256	301	346	391			0.5
32	77	122	167	212	257	302	347	392			1.0
33	78	123	168	213	258	303	348	393		45	1.5
34	79	124	169	214	259	304	349	394			2.0
35	80	125	170	215	260	305	350	395			3.0
36	81	126	171	216	261	306	351	396			0.5
37	82	127	172	217	262	307	352	397			1.0
38	83	128	173	218	263	308	353	398	5	60	1.5
39	84	129	174	219	264	309	354	399			2.0
40	85	130	175	220	265	310	355	400			3.0
41	86	131	176	221	266	311	356	401			0.5
42	87	132	177	222	267	312	357	402			1.0
43	88	133	178	223	268	313	358	403		75	1.5
44	89	134	179	224	269	314	359	404			2.0
45	90	135	180	225	270	315	360	405			3.0

utilized in these analyses. The results are presented in the form of moment-curvature, axial load-ultimate moment, axial load-ultimate curvature, and ductility factor-steel percentage diagrams under a broad range of combinations of the variables (italicized above).

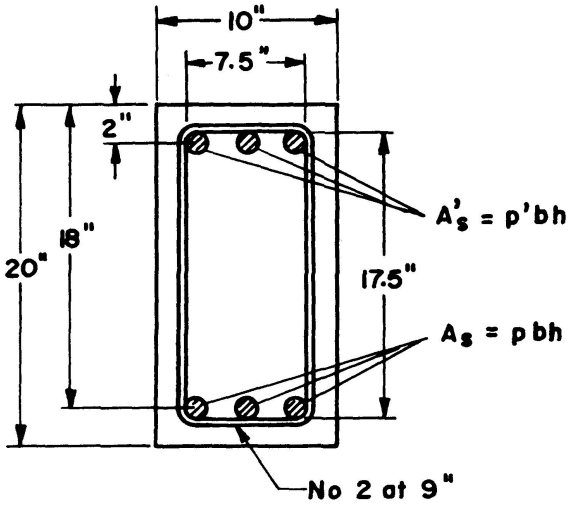

Fig. 1. Typical section used in analysis.

Effects of Axial Load on Moment-Curvature Diagrams

The M-ϕ diagrams of the sections analyzed are presented in Figs. 2 to 10. Each of these figures corresponds to a particular combination of concrete strength and steel grade and contains the diagrams corresponding to five different sectional reinforcement percentages. The curves in each diagram illustrate the effects of varying levels of axial load on nine identical sections.

The numerical values of moment and curvature at the stage of "yielding" and "sectional failure (ultimate)", associated with the M-ϕ diagrams in Figs. 2 to 10, the ratios of ultimate to yield moments, and of the corresponding curvatures, are important for subsequent discussion in this paper. It should be noted that, as in [8], the "yield" stage is defined as that at which the tension reinforcement in a section reaches its yield point stress and the "ultimate" stage is that at which the section reaches its moment carrying capacity (for a given axial load). This ultimate stage definition is different from the conventional one, according to which a section is assumed to have failed when the concrete strain in its extreme compression fibre reaches an arbitrary limiting value [3], [4], [5].

Tension, balanced and compression failures of a section are characterized by the yielding of tension reinforcement prior to, simultaneously with, and subsequent to the attainment of sectional moment carrying capacity, respectively. Sections subject to axial loading of magnitude below a certain level (corresponding to balanced failure) fail in tension. Figs. 2 to 10 indicate that the yield moments and curvatures of such sections increase with increasing levels of the axial loads. Both M_y and ϕ_y (corresponding to any given level of axial load) also increase with increasing steel percentages of the sections and with increasing reinforcement strengths. M_y increases somewhat, but ϕ_y remains unchanged, or decreases slightly, with increasing concrete strengths.

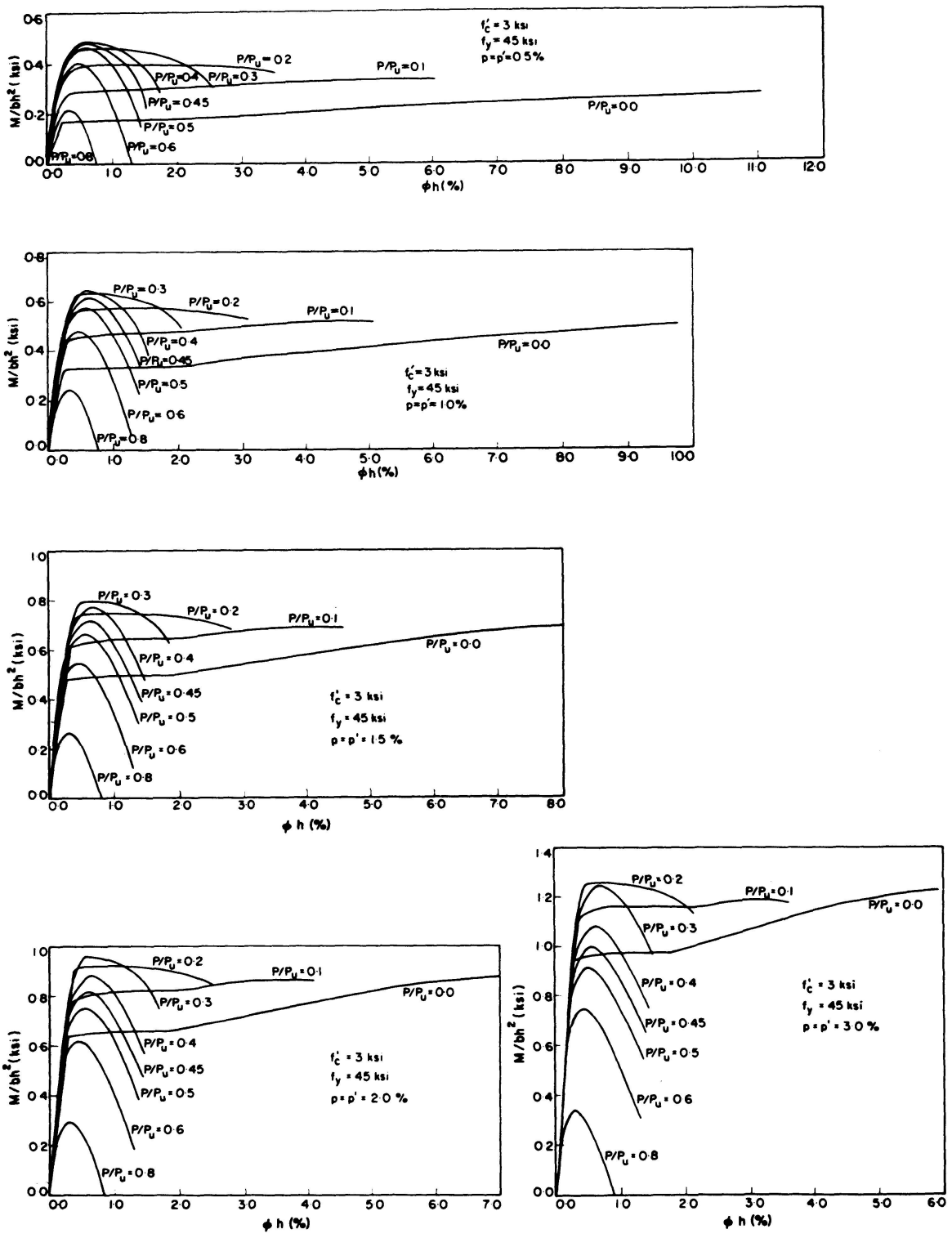

Fig. 2. M-ϕ diagrams, as affected by axial loads, for various concrete and steel grades and amounts of reinforcement ($f'_c = 3$ ksi, $f_y = 45$ ksi).

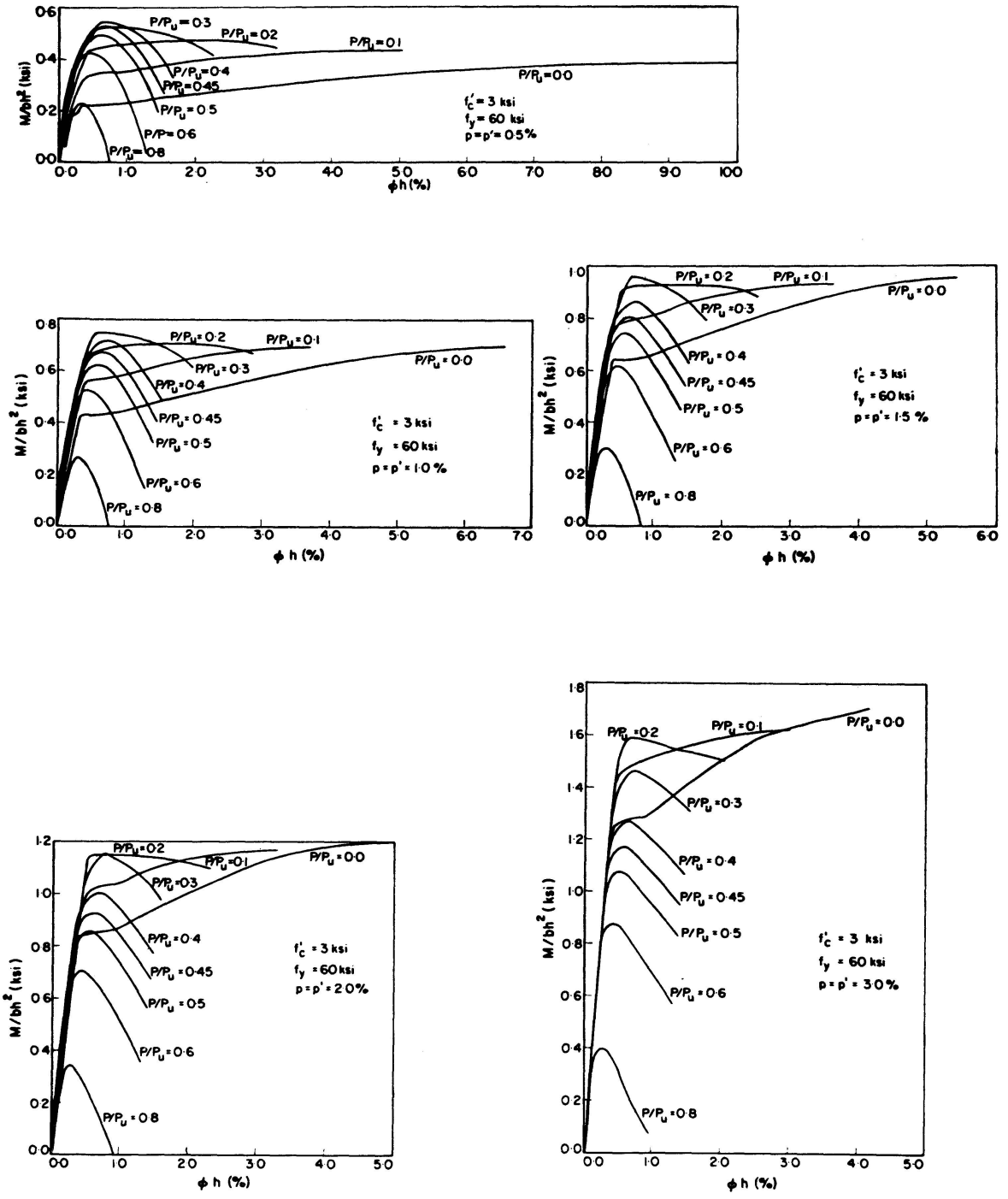

Fig. 3. M-ϕ diagrams, as affected by axial loads, for various concrete and steel grades and amounts of reinforcement ($f'_c = 3$ ksi, $f_y = 60$ ksi).

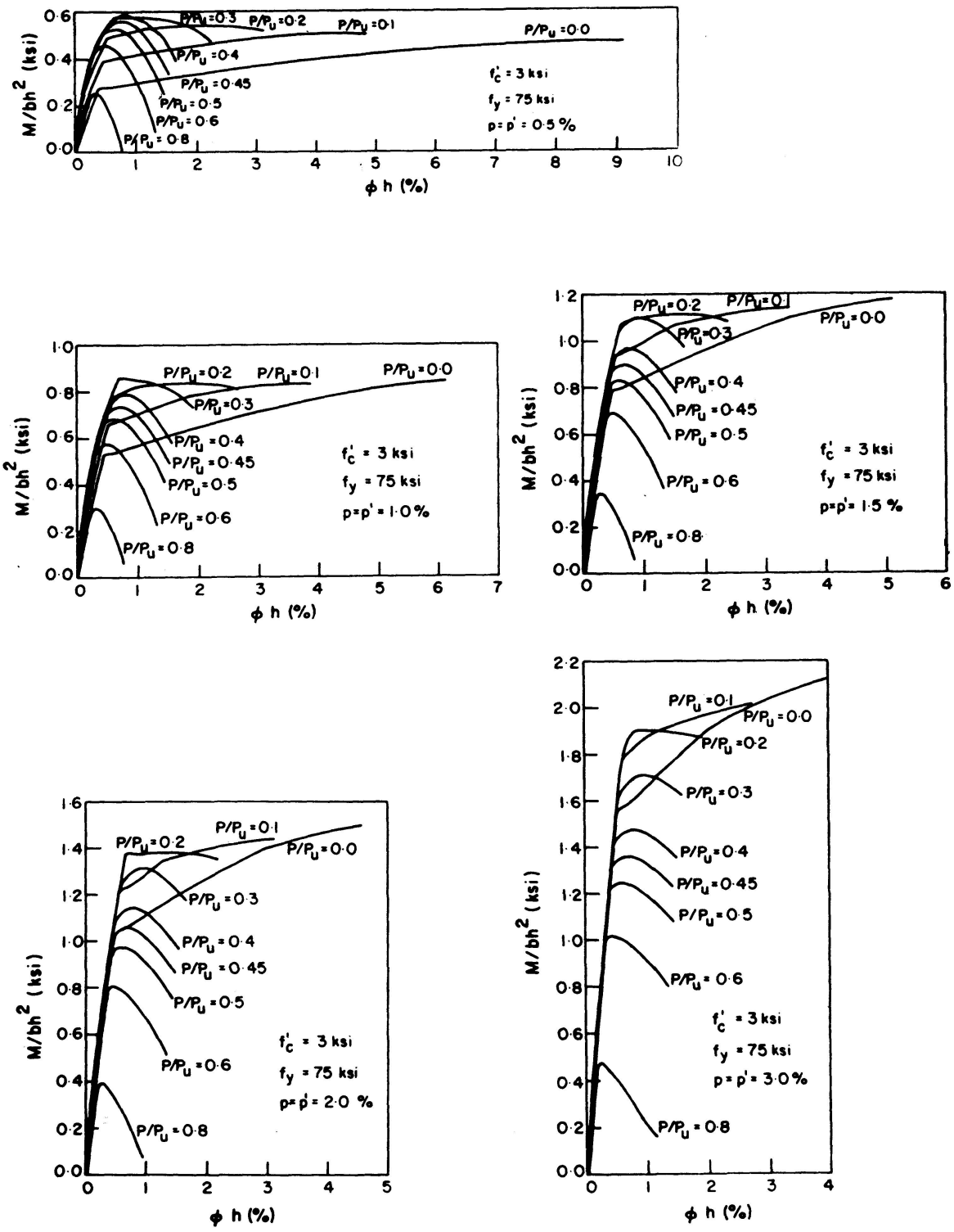

Fig. 4. M-ϕ diagrams, as affected by axial loads, for various concrete and steel grades and amounts of reinforcement ($f_c' = 3$ ksi, $f_y = 75$ ksi).

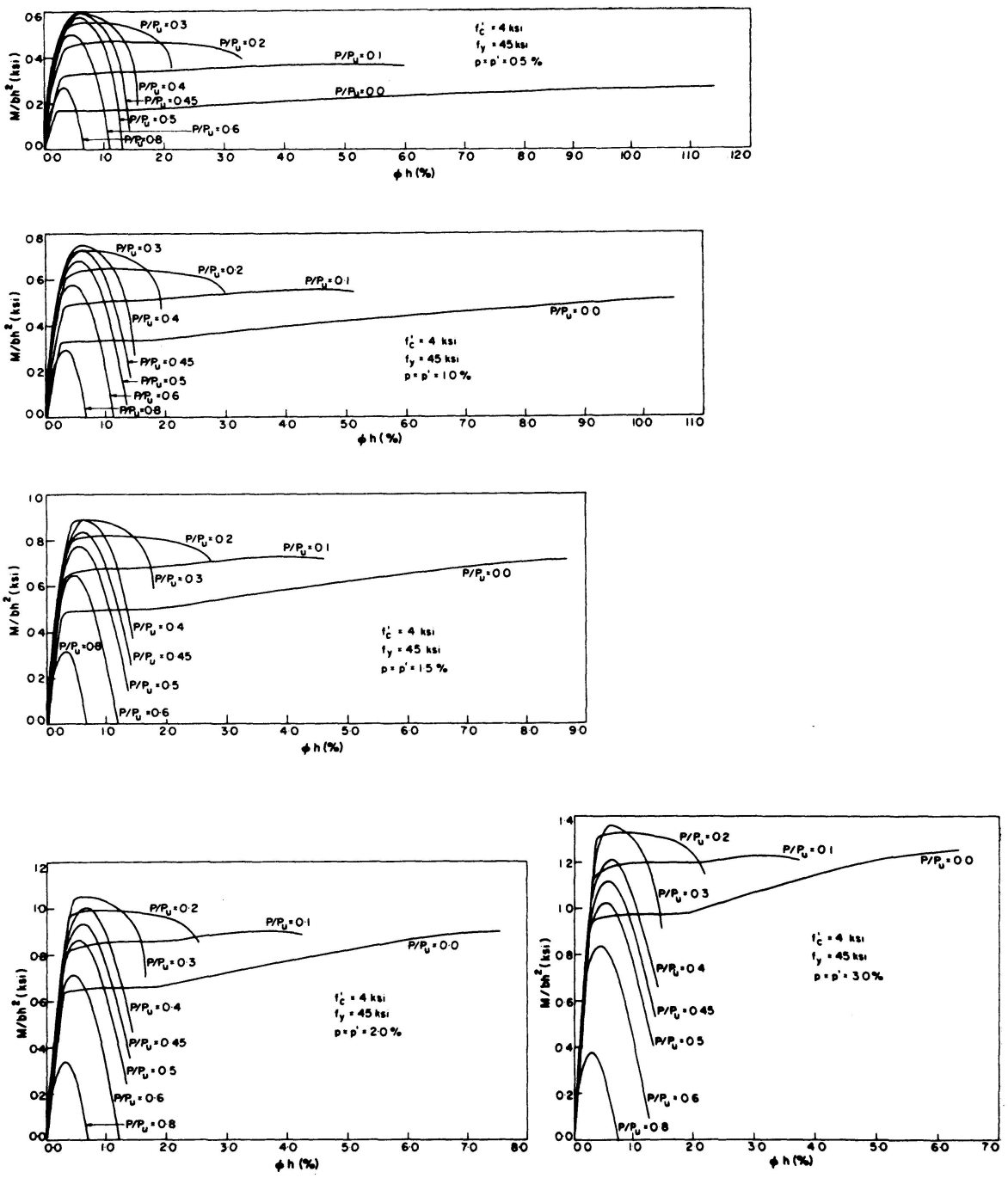

Fig. 5. M-ϕ diagrams, as affected by axial loads, for various concrete and steel grades and amounts of reinforcement ($f'_c = 4$ ksi, $f_y = 45$ ksi).

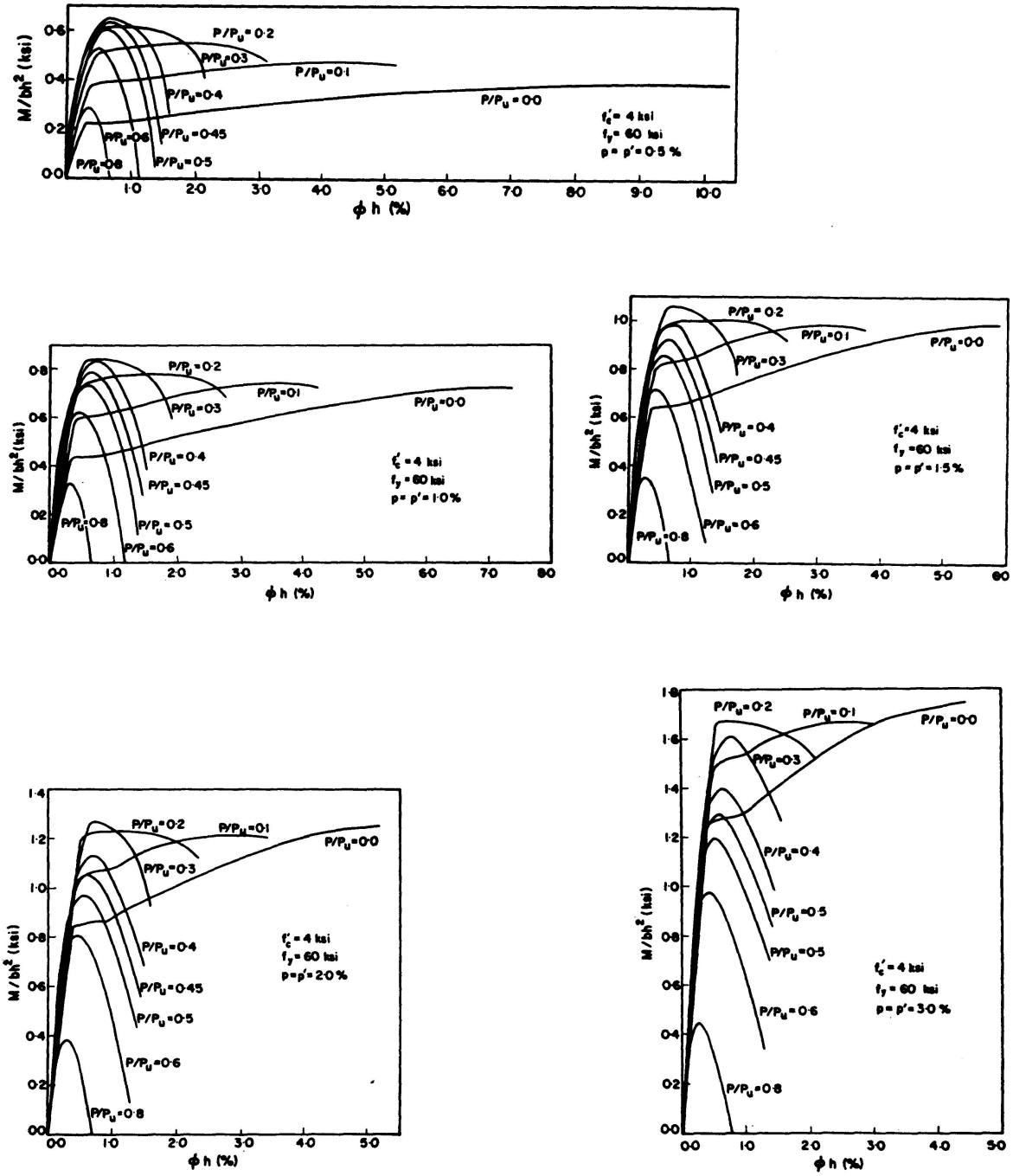

Fig. 6. M-ϕ diagrams, as affected by axial loads, for various concrete and steel grades and amounts of reinforcement ($f'_c = 4$ ksi, $f_y = 60$ ksi).

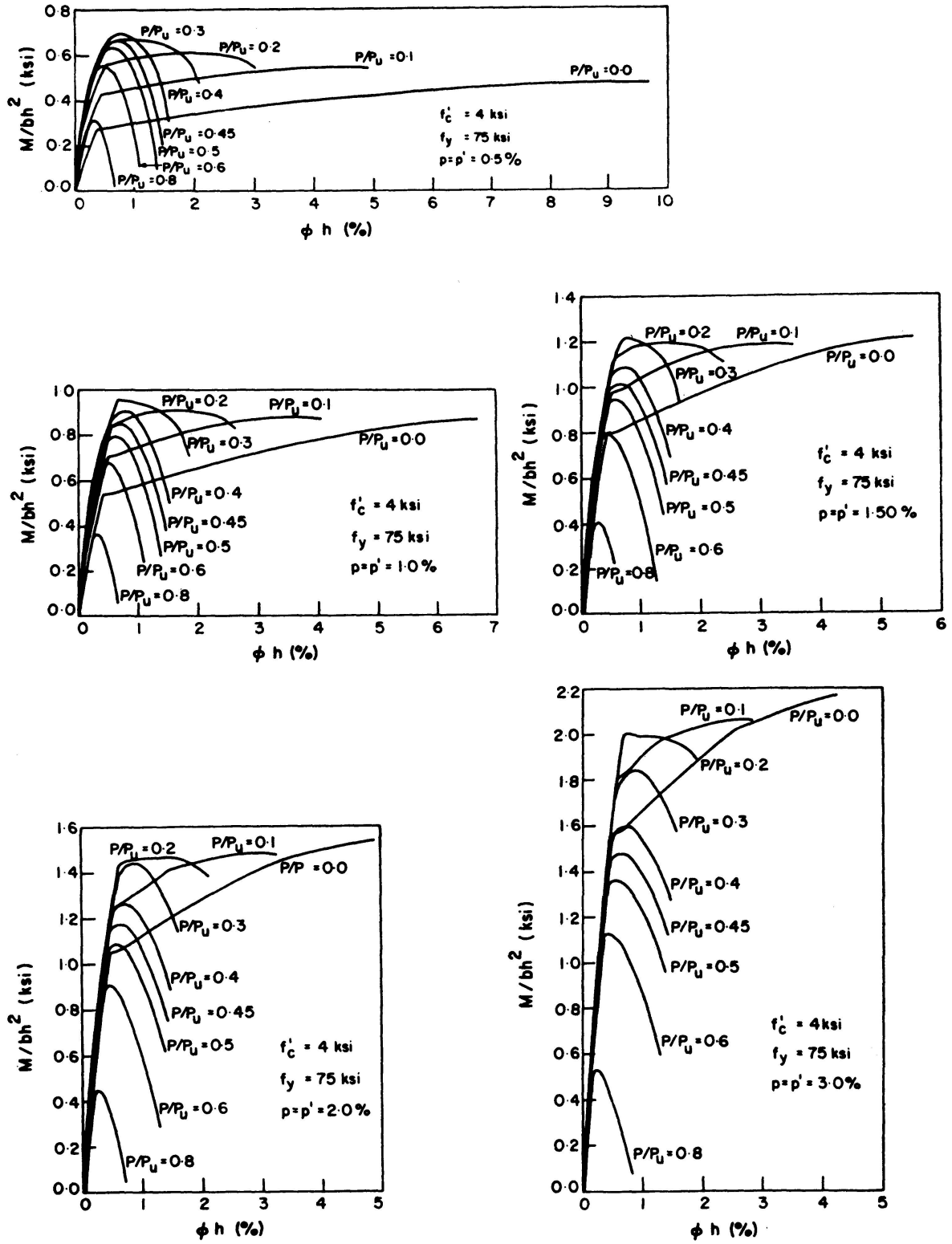

Fig. 7. M-ϕ diagrams, as affected by axial loads, for various concrete and steel grades and amounts of reinforcement ($f'_c = 4$ ksi, $f_y = 75$ ksi).

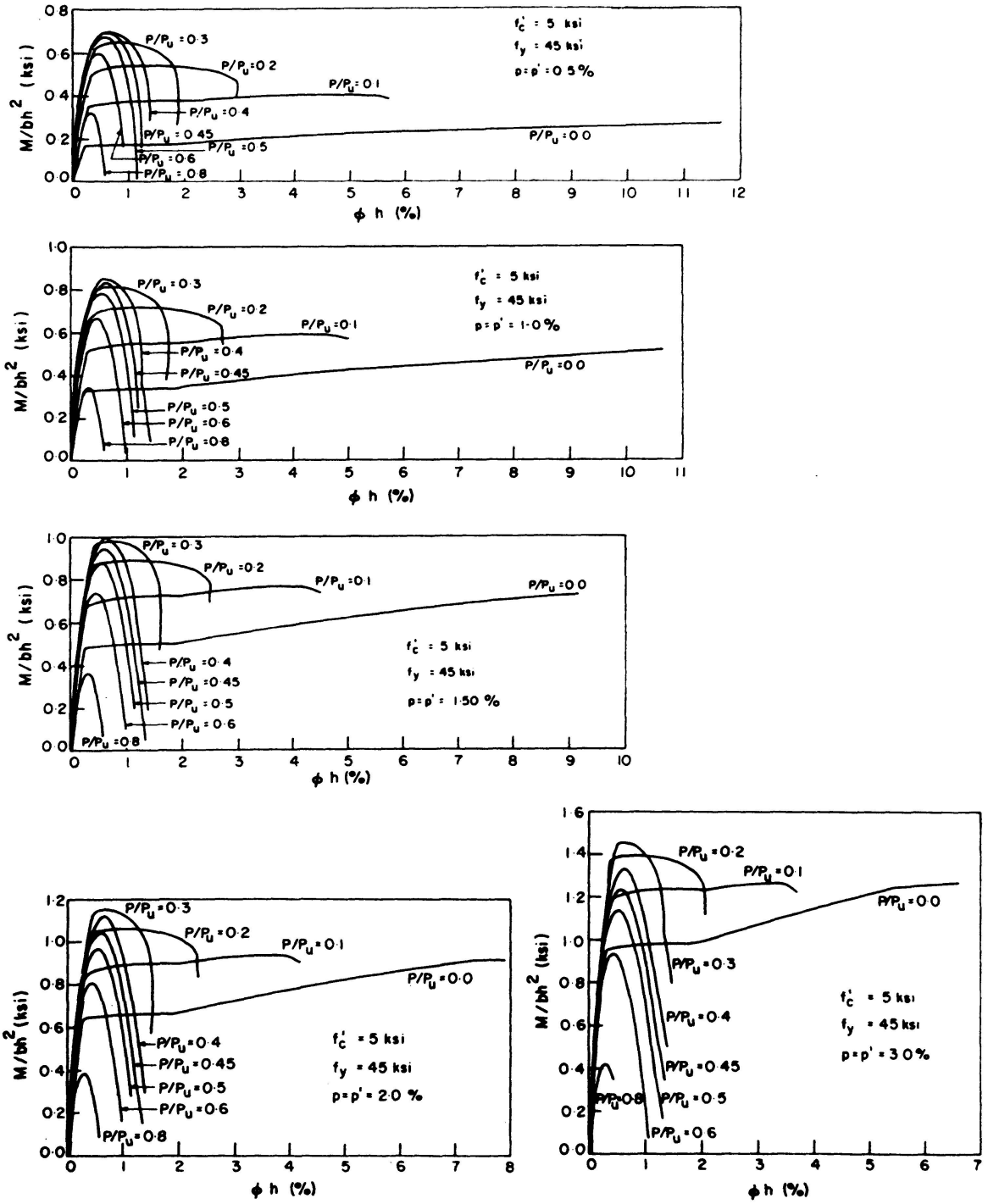

Fig. 8. M-ϕ diagrams, as affected by axial loads, for various concrete and steel grades and amounts of reinforcement ($f_c' = 5$ ksi, $f_y = 45$ ksi).

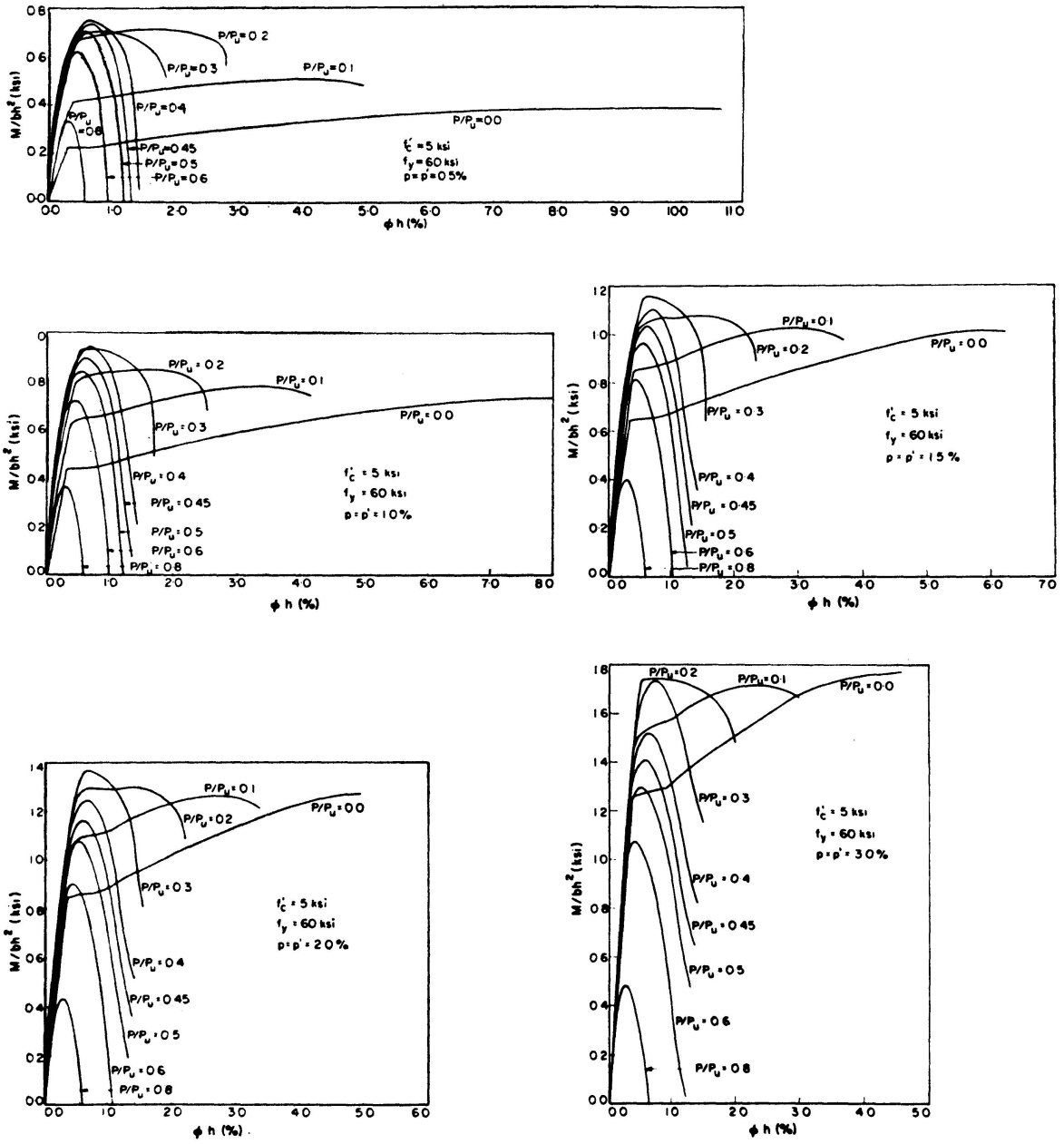

Fig. 9. M-ϕ diagrams, as affected by axial loads, for various concrete and steel grades and amounts of reinforcement ($f'_c = 5$ ksi, $f_y = 60$ ksi).

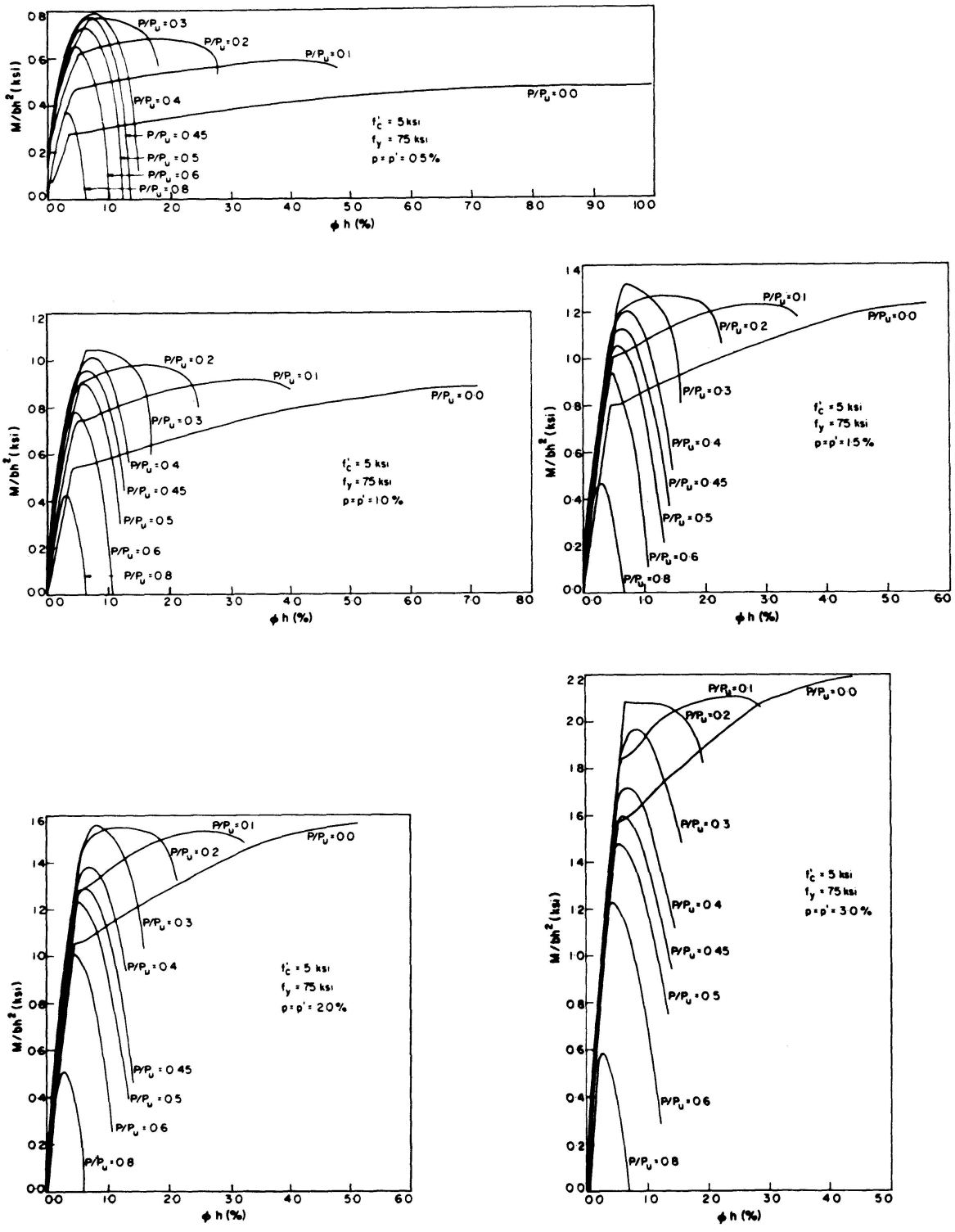

Fig. 10. M-ϕ diagrams, as affected by axial loads, for various concrete and steel grades and amounts of reinforcement ($f'_c = 5$ ksi, $f_y = 75$ ksi).

The effects of axial loading, of concrete and steel grades and amounts of reinforcement on M_u, ϕ_u, ϕ_u/ϕ_y and M_u/M_y are discussed in the next four sections.

Load-Moment Interaction Diagrams

The $P/P_u - M_u/b\,h^2$ interaction diagrams of Fig. 11 were plotted from the relevant data presented in Figs. 2 to 10. Fig. 11 consists of the diagrams corresponding to nine combinations of concrete and steel grades. Each of these diagrams contains the curves (in full lines) corresponding to five different sectional reinforcement percentages.

The break in each interaction diagram corresponds to the balanced failure conditions, above and below which are the compression and tension failure zones, respectively.

The shape of the interaction diagrams in the region corresponding to tension failure should be noted. This shape is a direct consequence of the ultimate stage definition adopted in this study. The interaction diagrams drawn in full lines change to the more familiarly shaped ones, indicated by dotted lines, if the ultimate stage is defined by the extreme compression fibre strain reaching a value of 0.3%.

From Fig. 11, it is apparent that the magnitude of the balanced load decreases with increasing steel percentages. This is contrary to an earlier finding by PFRANG et al. [4], who had concluded that the above magnitude was independent of reinforcement content. Fig. 11 also indicates that the balanced load decreases somewhat with increasing reinforcement strengths and decreases with increasing concrete strengths.

Fig. 11 shows that sectional moment capacity, corresponding to any given level of axial load, increases with increasing reinforcement percentage and steel and concrete strengths. If sectional failure is defined in a conventional manner (by a limiting compression concrete strain), the moment capacity of a section increases with increasing levels of axial load as long as failure is governed by tension, and thereafter decreases as the axial loads are further increased. The trend in the tension failure region changes if sectional failure is defined as in the present study, with moment carrying capacities under pure bending being larger than those under bending combined with low axial loads.

Axial Load-Ultimate Curvature Diagrams

The $P/P_u - \phi_u h$ diagrams in Fig. 12 were also plotted from the data presented in Figs. 2 to 10. To the left of each diagram (corresponding to a particular combination of steel and concrete grades) are the curves drawn according to the conventional definition of failure, and to the right are those plotted

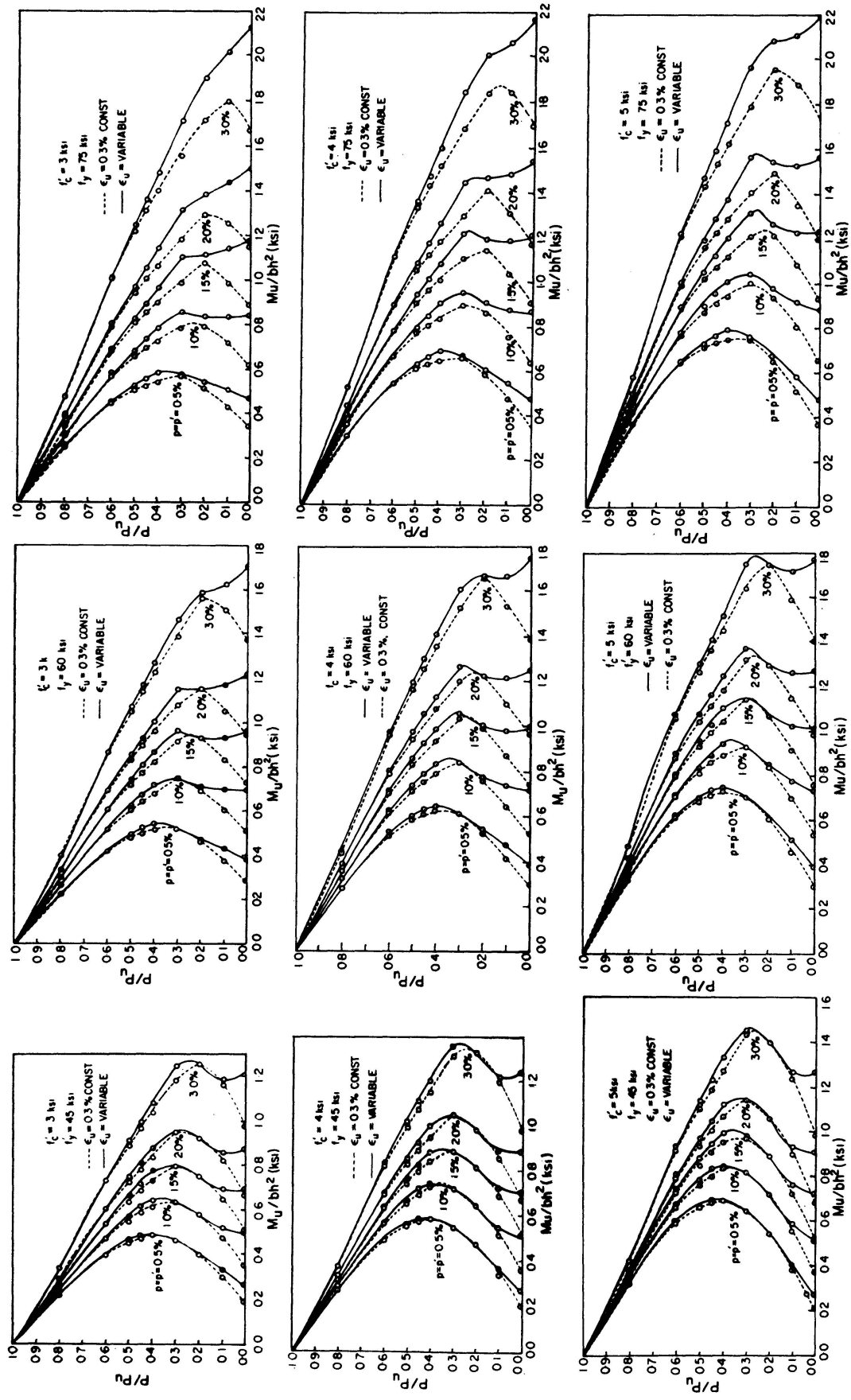

Fig. 11. Axial load-moment interaction diagrams for various concrete and steel grades, and amounts of reinforcement.

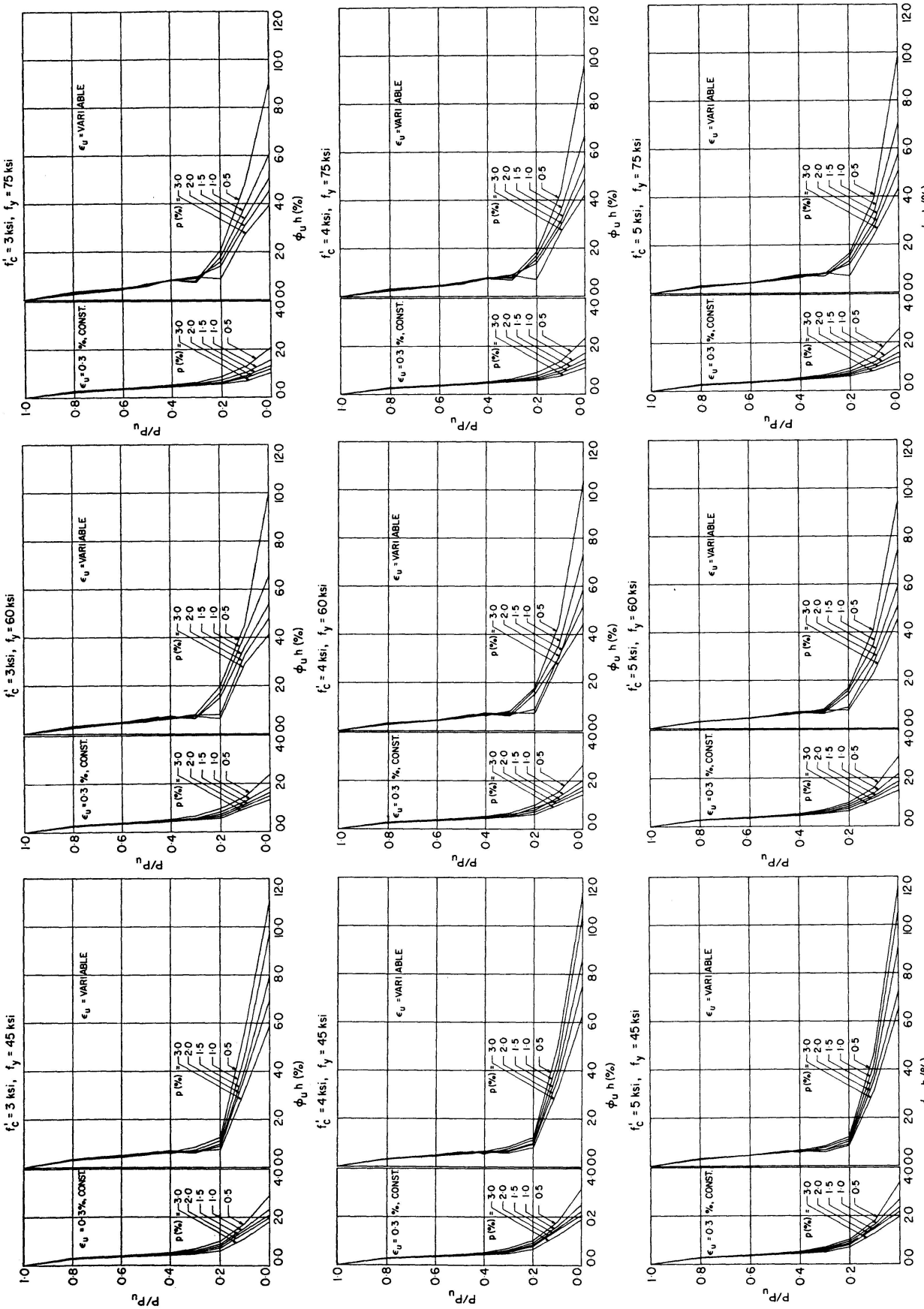

Fig. 12. Axial load-ultimate curvature diagrams for various concrete and steel grades, and amounts of reinforcement.

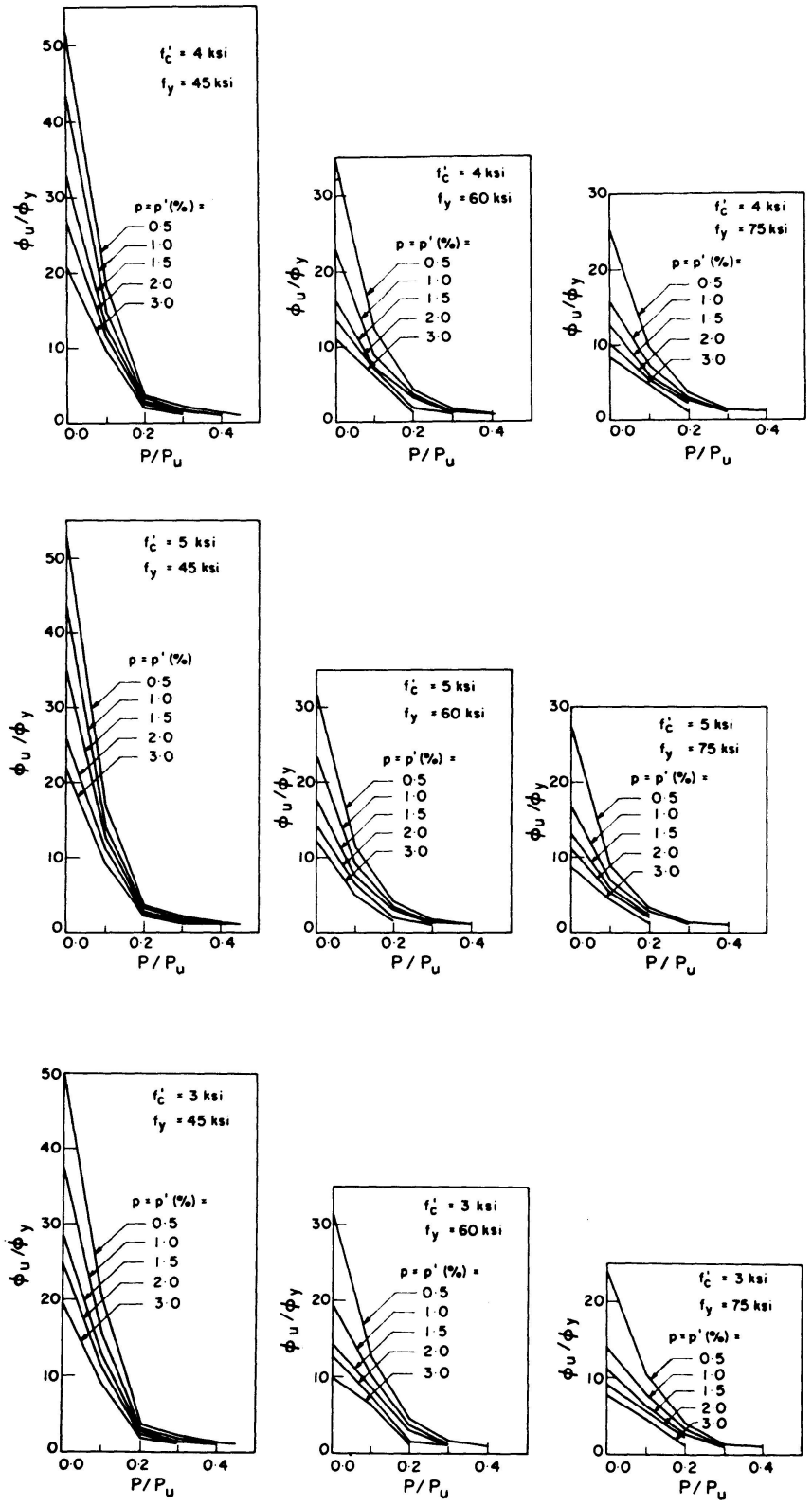

Fig. 13. Effects of axial loads on the ductility of reinforced concrete sections.

according to the failure definition of the present study (each curve corresponding to a particular sectional steel percentage). The conventional definition of failure, which provides a slightly conservative estimate of the moment capacity of a section (Fig. 11), obviously leads to a gross underestimation of its deformability. It is evident that the ultimate curvature decreases steadily with increasing levels of axial load, when failure is defined by a limiting strain. While this trend is generally true in case of the definition of failure adopted herein, some irregularities in the trend are observed around the balanced points. Ultimate curvatures (conforming to both definitions) are found to be extremely small in the regions of compression failure.

Fig. 12 shows that the ultimate curvature corresponding to any given axial load level decreases with increasing steel percentages of sections and with reinforcement strengths, and increases slightly with increasing concrete strengths.

Effects of Axial Load on Sectional Ductility

The ductility factor, defined as the ratio of ultimate to yield curvatures, ϕ_u/ϕ_y, is a satisfactory index of the ductility of reinforced concrete sections subject to pure and combined bending [8]. From the numerical data presented in Figs. 2 to 10, ductility ratio versus axial load curves corresponding to various reinforcement percentages are plotted in Fig. 13 for the nine combinations of steel and concrete grades considered. This figure and the tables indicate that as long as failure is governed by tension, a section is capable of mobilizing a certain amount of ductility, although this decreases drastically as the axial load on the section approaches the level corresponding to balanced failure. Fig. 13 also indicates that for the low levels of axial load usually carried by flexural members in reinforced concrete frames (not exceeding 10–15% of the axial load capacity), fairly high amounts of sectional ductility are always available.

It was observed in Ref. [8] that sectional ductility decreases with increasing steel percentages, increasing reinforcement strengths, and decreasing concrete strengths, a trend which is evident from Fig. 13.

Discussion of Results

a) Definition of Sectional Failure in Deformation Analysis

The ductility factor, defined as the ratio of ultimate to yield curvatures, ϕ_u/ϕ_y, is widely accepted as an index of the ductility of reinforced concrete sections subject predominantly to flexural action under static loading. However, while the yield curvature, ϕ_y, is generally defined as the curvature at which the tension steel reaches its yield point stress, several definitions of the

ultimate stage or the failure of a section, to which the curvature ϕ_u corresponds, are in use.

In most current codes of practice, ϕ_u is defined as the curvature at which a conventional limiting value of the concrete strain (corresponding presumably to the onset of crushing) is attained at the extreme compression fibre ($\epsilon_u = 0.3\%$ according to the ACI Code [11]). In this study ϕ_u has been defined as the curvature corresponding to the attainment of sectional moment capacity. A third definition of ϕ_u appears to be gaining increasing acceptance. "Many sections have considerable capacity for plastic rotation beyond the peak of the moment-curvature curve. It would seem reasonable to recognize some of this available deformation after maximum moment and to define ϕ_u as the curvature when the moment is reduced by some arbitrary amount after the maximum moment" [7]. ϕ_u was defined as the curvature corresponding to $0.9 M_u$ and M_y along the descending branch of the M-ϕ diagram in Refs. [7] and [12], respectively. The three definitions of ϕ_u discussed above are illustrated schematically in Fig. 14.

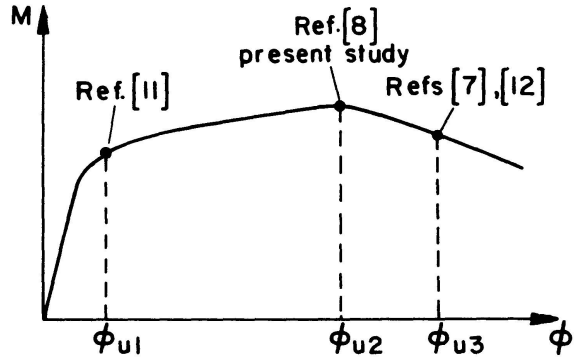

Fig. 14. Various definitions of ultimate curvature.

It has been noted earlier that the conventional definition of failure grossly underestimates the deformability of a section. Fig. 12 illustrates that the ratio ϕ_{u2}/ϕ_{u1} may be as large as 4–5 for sections failing in tension. A second disadvantage of this failure definition is that the limiting value of concrete strain at the extreme compression fibre has to be either arbitrarily fixed, or based on visual observations of the onset of crushing in experiments. The definitions of ϕ_u adopted in Refs. [7], [12] possibly account for the deformation capacity of a section to a fuller extent than the present study (depending upon sectional properties, ϕ_{u3} may be considerably larger than ϕ_{u2}). However, these definitions also are arbitrary. The failure of a section, as defined in the present study, corresponds to a mathematically well defined point, i.e. the peak of the M-ϕ diagram. The choice of this functional viewpoint is logical, noting that the primary purpose of a structural member is to carry loads. This definition is unlikely to prove unduly conservative in estimating the deformability of sections with current geometric and material properties. It is therefore recommended that, at least for the purposes of deformation analysis, sectional

failure be defined as the stage corresponding to the attainment of the maximum flexural capacity.

b) Definition of Sectional Failure in Strength Analysis

Fig. 11 shows that the strength of a section, unlike its deformability, is relatively insensitive to the definition of sectional failure. The dotted *P-M* interaction diagrams in Fig. 11, corresponding to the conventional definition of sectional failure (ultimate stage defined by $\epsilon_u = 0.3\%$), provide safe and only slightly conservative lower bounds on the moment capacities of sections subject to given levels of axial load.

It should be observed that the rather unusual shape of the tension failure regions of the *P-M* interaction diagrams for the definition of failure adopted in the present study (Fig. 11) was first noted by the authors [8]. The significance and implications of this shape are yet to be fully understood.

In view of the above, it is recommended that, pending further investigation, the conventional definition of failure be retained for strength analysis. It is hoped that future research will clarify all aspects of the functional definition of failure, leading to its wider acceptance. The arbitrariness of the conventional definition is not as much of a disadvantage in strength as in deformation analysis. The numerical value adopted for ϵ_u would normally have a relatively minor effect on sectional strength.

c) Estimate of Ductility Requirements in Design

Ductility governs the rotation capacity of hinging zones and the redistribution of moments in a structure; the adaptability of structures to foundation settlements and volume changes; and the energy absorption capacity of structures subject to dynamic (wind, earthquake, blast) loads. Ductility safeguards a structure against sudden overloads, impact and load reversals. For this reason it is necessary and desirable that structures be capable of mobilizing a reasonable level of ductility whenever actions such as those mentioned above are foreseen [8]. However, there have been very few attempts at determining the amount of ductility that may be required in structures designed to meet specific functional requirements. These limited attempts have largely been confined to the area of aseismic design.

A measure of the ductility of structures with regard to seismic loading is the displacement ductility factor defined as Δ_u/Δ_y, where Δ_u, Δ_y are the lateral deflections at the ultimate stage and at first yield, respectively. The commentary on the code of the Structural Engineers Association of California [13] indicates that the displacement ductility factor required in aseismic design may range from three to five. It is important to recognize the difference between the ratio Δ_u/Δ_y, and the index of sectional ductility, ϕ_u/ϕ_y. "Once

yielding has commenced in a frame the deformations concentrate at the plastic hinge positions and hence when a frame is deflected laterally in the post-elastic range the required ϕ_u/ϕ_y ratio at the plastic hinges is greater than the Δ_u/Δ_y ratio'' [7]. The following suggestion was offered in Ref. [7] *without* a rigorous basis: "Columns capable of reaching a curvature ductility factor ϕ_u/ϕ_y of at least 15, with ϕ_u defined as the curvature when the moment has reduced to 80–90 percent of the maximum moment, would appear to be a reasonably practical approach to column design for seismic resistance.'' It is obvious that the required ϕ_u/ϕ_y would be less than 15 if ϕ_u is defined as the curvature corresponding to M_u, rather than to $0.8\text{–}0.9\,M_u$.

A more precise estimate of the sectional ductility required in structures would require a considerable amount of further research, and is beyond the scope of the present study. The emphasis here is on determining the amounts of ductility that may be available in column sections with varying concrete and steel grades and amounts of reinforcement.

d) Amounts of Available Ductility

ACI 318-71 [11] requires that the column ends in ductile moment-resisting frames be provided with special transverse reinforcement when the column load exceeds 40% of the load corresponding to balanced failure. Therefore, $0.4\,P_b$ can be considered as the highest axial load to which a column section without any special lateral reinforcement may be subjected.

Table 2. Ratios of balanced to ultimate axial loads for various concrete and steel grades and reinforcement percentages

	f'_c = 3 ksi			f'_c = 4 ksi			f'_c = 5 ksi		
	f_y = 45 ksi	60 ksi	75 ksi	f_y = 45 ksi	60 ksi	75 ksi	f_y = 45 ksi	60 ksi	75 ksi
$p=p'=0.5\%$	0.40	0.35	0.30	0.40	0.37	0.32	0.40	0.40	0.35
$p=p'=1.0\%$	0.32	0.30	0.24	0.35	0.29	0.30	0.36	0.30	0.30
$p=p'=1.5\%$	0.30	0.25	0.20	0.30	0.27	0.20	0.33	0.28	0.24
$p=p'=2.0\%$	0.29	0.20	0.20	0.30	0.24	0.20	0.30	0.26	0.20
$p=p'=3.0\%$	0.20	0.20	0.10	0.24	0.20	0.15	0.27	0.20	0.20

The ratios P_b/P_u for the sections considered in the present investigation are listed in Table 2. These ratios were determined from the dotted interaction diagrams in Fig. 11, which correspond to sectional failure defined by $\epsilon_u = 0.3\%$. The amounts of ductility available in sections with varying combinations of the variables studied and subject to $P = 0.4\,P_b$ were determined from Fig. 13. Table 2 was used to convert the fixed P/P_b ratio of 0.4 to the appropriate P/P_u ratios. The results of this analysis are presented in Table 3. Table 3

Table 3. Ductility available in sections with varying concrete and steel grades and reinforcement percentages, and subject to 40% of balanced axial load

	f'_c = 3 ksi			f'_c = 4 ksi			f'_c = 5 ksi		
	f_y = 45 ksi	60 ksi	75 ksi	f_y = 45 ksi	60 ksi	75 ksi	f_y = 45 ksi	60 ksi	75 ksi
$p=p'=0.5\%$	10.5	9.5	9.0	9.5	8.4	8.0	8.8	7.0	6.5
$p=p'=1.0\%$	12.0	9.0	8.0	10.1	8.0	6.5	9.0	8.0	6.0
$p=p'=1.5\%$	11.0	8.5	7.3	10.7	7.0	7.5	9.5	7.0	6.2
$p=p'=2.0\%$	10.0	8.5	6.3	9.5	7.3	6.5	9.3	6.3	6.3
$p=p'=3.0\%$	11.0	7.0	6.5	10.0	7.0	6.0	8.7	6.5	5.0

shows that reinforced concrete sections, subject to the highest axial loads permitted by the ACI code [11], possess a minimum ductility ratio of 5 under the most adverse variable combinations studied. The ratio may be as high as 12 under more favourable combinations of the variables.

Conclusions

1. The magnitude of the balanced axial load, which separates tension from compression failure, decreases with increasing reinforcement percentages, increasing reinforcement strengths, and decreasing concrete strengths.

For the large number of section investigated, the above magnitude neither exceeded 40%, nor ever fell below 20% of the axial load capacities of the sections (these values are not unduly sensitive to the adopted definition of sectional failure).

2. If sectional failure is defined in a conventional manner in terms of limiting compression concrete strains, ultimate moments increase with increasing levels of axial load, as long as failure is governed by tension, and thereafter decrease as the axial loads are further increased. The corresponding curvatures decrease steadily with increasing levels of axial load.

If failure is defined, as in the present study, in terms of sectional moment capacity, two irregularities are found in the above trends, which otherwise remain generally valid. Firstly, moment capacities under pure bending are found to be larger than those under bending combined with low axial loads. Secondly, ultimate curvatures are sometimes found to increase with increasing axial loads around the balanced point.

3. It appears reasonable to define the failure of a section as the stage corresponding to the attainment of: (a) sectional moment capacity in deformation analysis, and (b) a limiting value of concrete strain at the extreme compression fibre in strength analysis.

4. Reinforced concrete sections without any special transverse reinforce-

ment, and subject to the highest axial loads permitted under the ACI code, i.e. $P=0.4P_b$, possess a ductility ratio of 5 under the most adverse, and of 12 under the most favourable, of the variable combinations studied.

5. Inelastic action, at least to an extent which would not require ductility in excess of the amounts indicated in Fig. 12, may be permitted in reinforced concrete column sections.

Notation

A_s = cross-sectional area of tension reinforcement.
A'_s = cross-sectional area of compression reinforcement.
b = width of section.
f'_c = standard cylinder strength of concrete.
f_y = yield strength of steel.
h = total depth of section.
M = sectional moment.
M_u = ultimate moment.
M_y = yield moment.
p = ratio of tension reinforcement area to gross area of section.
p' = ratio of compression reinforcement area to gross area of section.
P = axial load on section.
P_b = balanced axial load.
P_u = ultimate axial load.
Δ_u = lateral deflection in a structure at ultimate stage.
Δ_y = lateral deflection in a structure at yield stage.
ϵ_u = concrete strain in extreme compression fibre at ultimate stage.
ϕ = sectional curvature.
ϕ_u = curvature corresponding to ultimate moment.
ϕ_y = curvature corresponding to yield moment.

Acknowledgement

This paper is based on a portion of the doctoral dissertation of the first author and is part of an investigation on the "Inelastic Behaviour of Reinforced Concrete Structures" in progress in the Solid Mechanics Division and the Department of Civil Engineering, University of Waterloo, Waterloo, Ontario, Canada, under the direction of the second author.

The financial support of the National Research Council of Canada, under Grants A-4789 and D-10, is gratefully acknowledged.

References

1. American Concrete Institute: Reinforced Concrete Design Handbook. 3rd. Ed., ACI 317, Detroit, Mich., 1965.
2. Whitney, C. S., and Cohen, E.: Guide for Ultimate Strength Design of Reinforced Concrete. ACI Journal, Proceedings, Vol. 53, No. 5, November 1956, p. 455–490.
3. Blume, J. A., Newmark, N. M., and Corning, L. H.: Design of Multi-story Reinforced Concrete Buildings for Earthquake Motions. Portland Cement Association, Skokie, Ill., 1961.
4. Pfrang, E. O., Siess, C. P., and Sozen, M. A.: Load-Moment-Curvature Characteristics of Reinforced Concrete Cross Sections. ACI Journal, Proceedings Vol. 61, No. 7, July 1964, p. 763–778.
5. Newmark, N. M., and Hall, W. J.: Dynamic Behavior of Reinforced and Prestressed Concrete Buildings under Horizontal Forces and Design of Joints (Incl. Wind, Earthquake, Blast Effects). Preliminary Publication, 8th Congress, IABSE, New York, September 1968, p. 585–613.
6. Sampson, R. A.: Ductility of Reinforced Concrete Columns. Master of Engineering Report, Univ. of Canterbury, Christchurch, New Zealand, 1971, 51 p.
7. Park, R., and Sampson, R. A.: Ductility of Reinforced Concrete Column Sections in Seismic Design. ACI Journal, Proceedings, Vol. 69, No. 9, September 1972, p. 543–550.
8. Cohn, M. Z., and Ghosh, S. K.: Flexural Ductility of Reinforced Concrete Sections. Publications, IABSE, Vol. 32, Part II, Zürich, 1972, p. 53–83.
9. Ghosh, S. K.: Some Aspects of the Nonlinear Analysis of Reinforced Concrete Structures. Ph. D. Thesis, Univ. of Waterloo, Waterloo, Ont., Canada, September 1972.
10. Sargin, M.: Stress-Strain Relationships for Concrete and the Analysis of Structural Concrete Sections. Study No. 4, Solid Mechanics Division, Univ. of Waterloo, Ont., Canada, 1971.
11. American Concrete Institute: Building Code Requirements for Reinforced Concrete. ACI 318-71, Detroit, Mich., 1971.
12. Srinivasa Rao, P., Kannan, P. R., and Subrahmanyam, B. V.: Influence of Span Length and Application of Load on the Rotation Capacity of Plastic Hinges. ACI Journal, Proceedings Vol. 68, No. 6, June 1971, p. 468–471.
13. Structural Engineers' Association of California Seismology Committee: Recommended Lateral Force Requirements and Commentary. San Francisco, Calif., 1968 (with 1970 amendment).

Summary

An investigation into the effects of axial load on the load-deformation characteristics of reinforced concrete sections is reported. The variables studied, besides the level of axial loading, are the concrete strength, steel grade, and amount of sectional reinforcement. The approach used is a computer simulation of the behaviour of over four hundred sections under a broad range of combinations of the above variables. The results are presented in the form of moment-curvature, axial load-ultimate moment, axial load-ultimate curvature, and ductility factor-axial load diagrams. The study provides a broad understanding of inelastic action in reinforced concrete columns subject to combined bending and compression.

Résumé

On présente une étude sur les influences de l'effort normal sur les caractéristiques de déformation de sections en béton armé. Les variables étudiées sont, à côté de l'intensité de la charge, les tensions dans le béton, la qualité de l'acier et le degré d'armature. La méthode utilisée est une étude par simulation sur computer du comportement de plus de quatre cents sections soumises à un grand nombre de combinaisons des variables ci-dessus. Les résultats sont présentés sous forme de courbes «moment-courbure», «effort axial-moment de rupture», «effort axial-courbure à la ruine» et «coefficient de déformabilité-effort axial». L'étude a permis une meilleure compréhension des phénomènes inélastiques dans les colonnes en béton armé soumises à un effort normal avec flexion.

Zusammenfassung

Es wird eine Untersuchung der Effekte von Axiallast-Deformations-Charakteristiken an Stahlbetonquerschnitten beschrieben. Die Variablen, die neben der Grösse der Axiallast untersucht werden, sind der Betonwiderstand, die Stahlqualität und die Grösse des Bewehrungsgrades.

Die benützte Näherungsmethode ist eine Computer-Simulation des Verhaltens von mehr als 400 Querschnitten unter einem breiten Spektrum von Kombinationen der obengenannten Variablen. Die Resultate werden in Form von Momenten-Krümmungen, Axiallast-Fliessmoment, Axiallast-Fliesskrümmung und Duktilitätsfaktor-Axiallast-Diagrammen angegeben. Die Studie vermittelt ein breites Verständnis über das inelastische Verhalten von Stahlbetonstützen unter kombinierter Biegung und Druck.